

Body and Surface Wave Seismic Tomography for Regional Geothermal Assessment of the Western Great Basin

Glenn Biasi¹, Leiph Preston², and Ileana Tibuleac¹

¹Nevada Seismological Laboratory, University of Nevada Reno, Reno NV

²Sandia National Laboratory, Albuquerque, NM

Keywords

Seismic imaging, regional seismic velocity structure, regional geology, Carson Sink

ABSTRACT

We present P-wave tomographic images of the shallow crust and discuss correlations of notable velocity anomalies with tectonic and structural elements of the Western Great Basin. Low velocities are identified in a closed contour on the south edge of the Carson Sink. This anomaly is interpreted to reflect the tectonic complexity in this area. Northwest dipping normal faults of the southern Stillwater Range intersect with NW-trending strike-slip faults of the eastern Walker Lane. We infer that at depth this mechanical incompatibility creates space, reflected at the surface in basin formation, and at depth by wide-spread fracturing that reduces body-wave velocity. Fracturing is probably responsible for a subtle NE-trending velocity reduction beneath the Mina Deflection. The value of the inversions will be their application to areas where the geology and tectonics are not as well understood. We also present new tomographic inversions of surface wave dispersion curves developed from earthquake and ambient noise sources. Model layers at 5.5 and 7 second periods are shown. At 5.5 seconds lower Raleigh wave group velocities in several cases parallel larger sedimentary basins. This effect is less pronounced for 7 second period waves. At this period waves are averaging over approximately the upper 7 km or so, and reflect to a greater degree the wave speed of basement rock beneath the basins. Integration of these complimentary sources of information has only just begun, but results seem likely to provide meaningful constraints and background information for use in regional geothermal assessment.

P-Wave Velocity in the Western Great Basin

First inversions of local and regional P- and S-wave arrival times have been developed from seismic data recorded by Nevada permanent networks and the temporary station occupation of the

Earthscope Transportable Array (TA) in Nevada and the western Great Basin (Figure 1, triangles on a coarse grid). Permanent coverage of the Nevada seismic networks is strongly concentrated in the western part of the state and in eastern California, so the additional coverage has been essential for developing meaningful regional images. P- and S-wave arrival times are identified by hand using a combination of Nevada seismic network processing and dedicated student effort. Our initial tomographic models use 5500 P arrivals and over 1300 S arrivals.

Figures 1a and 1b show model P-wave velocities at depths of 5 and 10 km as transparency layers over topography. Coverage at both depths is best in the west where station density is highest, and with the event coverage used, is too sparse in the east to return a resolved image. A number of features appear to correlate with known geologic structures. "PSN" is a slightly extended proto-Sierra Nevada terrain consisting of Jurassic and Cretaceous basement rocks of Sierran affinity that seem to comprise an island between the more extended Black Rock and Carson Sink regions. The Carson Sink (CS) appears as a prominent low velocity closure. There is a suggestion that the low velocities at 10 km depth are slightly farther south, for reasons that are unknown at the moment. The Sierra block is clearest in the 5 km layer. This may be because the rocks are less fractured and more geologically homogeneous than any similar-sized terrain to the east. Also, the upper 5 km reflect the extremes of surficial geology to a greater degree than 10 km and deeper. This effect may be seen by comparing the number and range of extremes in seismic velocity in the 5 km layer to the relatively more sedate 10 km depth layer. The low velocity area southeast of the "SJ" label on the 5 km and 10 km layers corresponds geographically with Scottys Junction. This area corresponds with a terrain of Precambrian and Paleozoic rocks bounded on the south by a network of older faults on locally in an EW orientation. On the 10 km depth layer, "LC" is a more speculative correlation of low velocities with the Lunar Crater volcanics west of Railroad Valley. "OV" marks a lineation of low velocities at the apparent northern confluence of the Owens Valley and Panamint-Saline Valley extensional systems. This velocity contrast appears from its shape and orientation to be structurally controlled.

Surface Wave Velocity Inversion

Surface waves provide a second, semi-independent source of wave speed indicators. Over 3000 Rayleigh dispersion curves have been developed from local and regional sources, supplemented by Rayleigh Green's functions from inter-station ambient noise cross-correlation. Dispersion curves provide estimates of seismic wave speed versus depth, with information about shallowest depths corresponding to the highest frequencies. In this phase of the project we invert these dispersion curves in a surface wave tomographic model. Resolution is generally lower than for body waves, but because surface waves sample the shallower crust, data are complimentary to results from body waves.

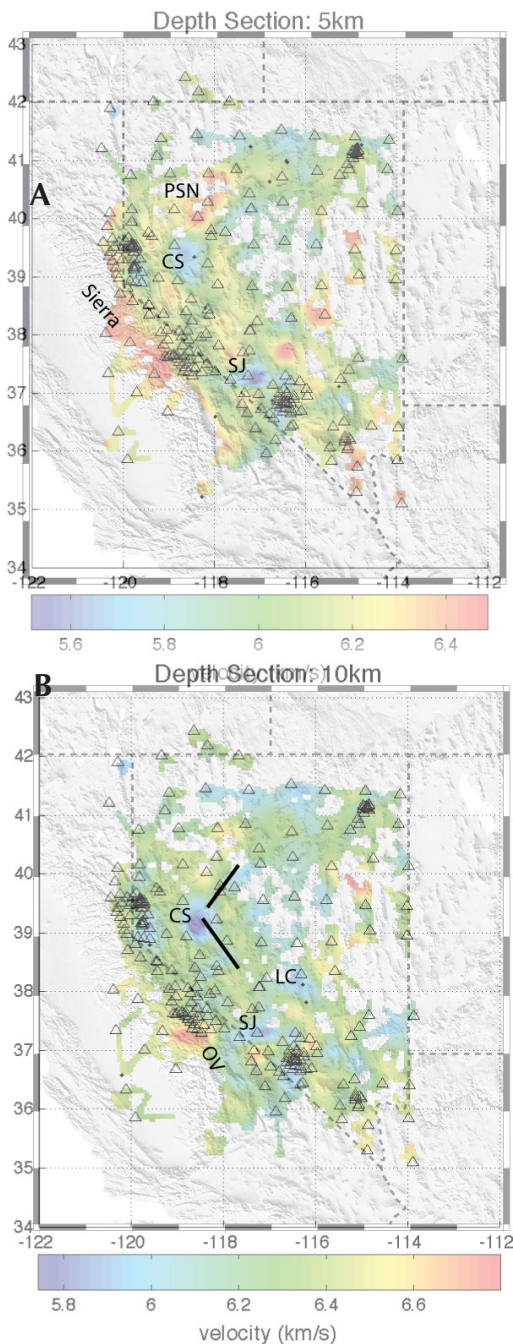


Figure 1. P-wave tomographic velocity model results for 5 and 10 km depth slices. Triangles mark seismic stations. Stations on a coarse grid most easily seen in northern and eastern Nevada are from the Earthscope Transportable Array. See text for labeling and further explanation.

Raleigh Wave Data

We analyze 2100 dispersion curves, developed from both single station and station-station pairs. Of these, 1759 are dispersion curves at distance greater than 15 km. The path coverage for the current analysis is shown in Figure 2. The dispersion curves are used to derive a preliminary tomographic model.

The group velocity tomography code we are using requires the sources and stations be within the region of interest (32° N to 45.6° N and 123.6° W to 110° W). We can use information from earthquakes located outside this area if we use differential dispersion curves, defined as inter-station dispersion curves estimated for stations 'in line' with an earthquake. To date, however, two-station dispersion curves have not been incorporated.

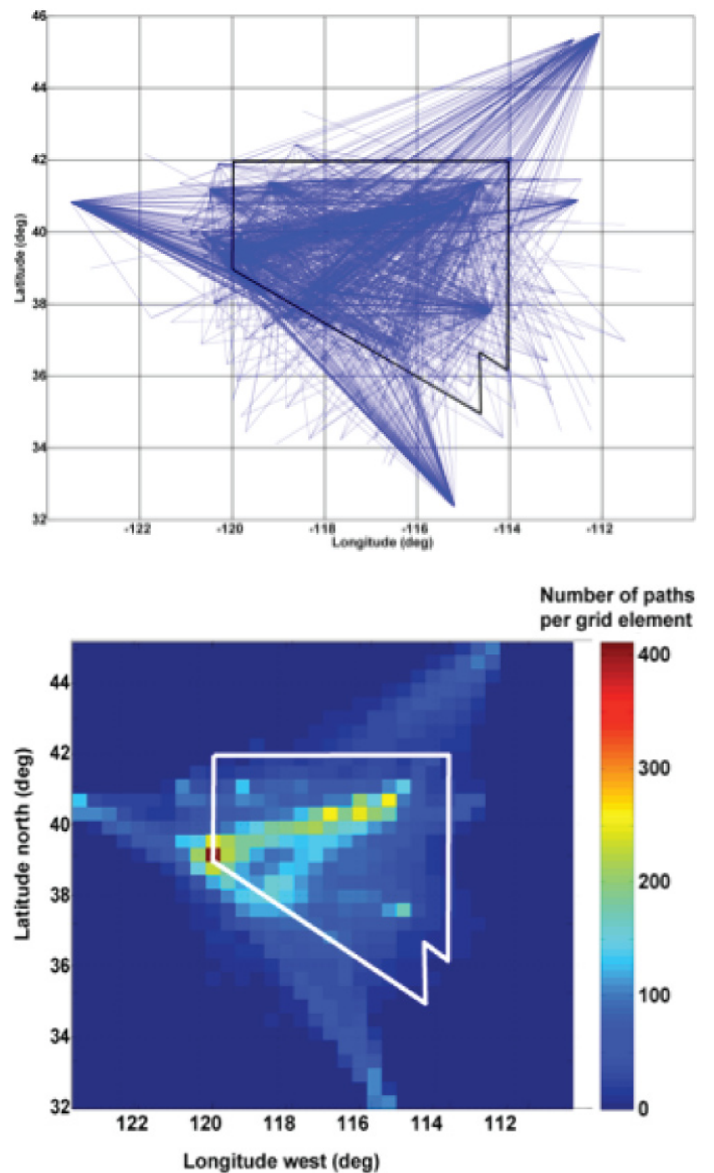


Figure 2. (Upper) The ray paths (more than 1700) for which first mode Rayleigh wave dispersion curves are estimated, from earthquakes and from ambient noise. The Nevada state line is shown in black. (Lower) Ray density in model blocks. The Wells, Nevada earthquake sequence provides good coverage for the geothermally important north-central part of the state.

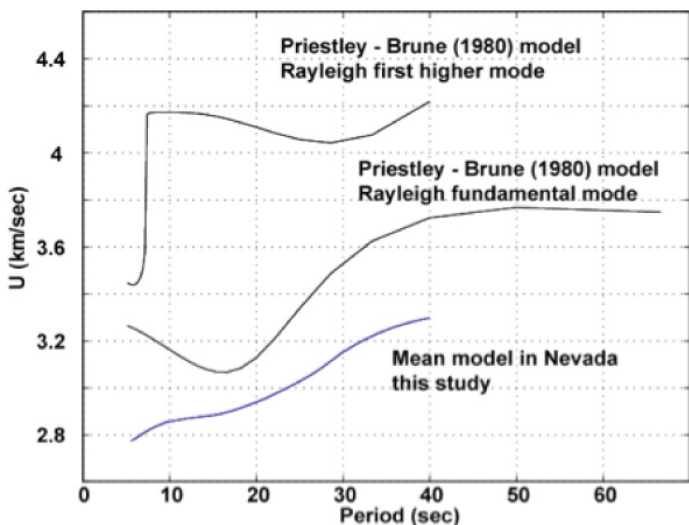


Figure 3. Dispersion curves for the fundamental and first higher Rayleigh mode derived from the Priestley and Brune (1982) shear velocity model in Nevada are shown in black. The mean model from all the dispersion curves we used is shown in blue.

Fundamental Mode Rayleigh Group Velocity Tomography

To estimate a preliminary group velocity tomographic model we use the code *gridsp*, written by Dr. Hafidh Ghalib. The code performs grid-dispersion inversion. Given the dispersion curves of surface waves over varying tectonic units, the pure-path dispersion curves are determined for each grid block or element (Feng and Teng, 1983). We use a grid of 0.4 deg (~44 km) for the preliminary model. The mean dispersion curve obtained from all measurements is shown in Figure 3.

Figure 4 presents surface wave tomographic inversion results for 5.5 and 7 second period waves. These waves sample the upper crust, with greatest sensitivity to the upper 5 to 7 km. Several low-velocity trends especially in the 5.5 sec inversion parallel major valley structures, especially in the north and west parts of Nevada. Sediments in the valleys would seem be primarily responsible for

this correlation, since surface wave velocities are more sensitive to shallow structure than to deep.

Discussion

Velocity contrasts presented in Figure 1 are difficult to interpret in the abstract, and we do not plan a detailed analysis until new TA data are incorporated and inverted. In the present map, however, a few observations can be made. On the 10 km layer short black lines have been drawn parallel to the structural fabric near the Carson Sink. The NW trending line approximately marks the eastern limit of NW strike-slip faulting that includes the Walker, Pilot Mountain, and Bettle’s Well faults. The NE trending line parallels the range front of the Stillwater Range, which, on its south end, hosts a system of down-to-the-northwest normal faults. The geometry of this system suggests that velocity anomaly here is probably not due to the rock itself, but is more likely a consequence of the structure. A first contribution to reducing P-wave velocity is the likely state of pervasive fracturing near the intersection of the NE and NW trending faults. The senses of stress in this fault system are inconsistent between the normal and strike-slip faults, requiring an accommodation zone of fractured rock. Strike-slip motion will contribute to deepening the southern Carson Sink where strike-slip motion transfers west in a trans-tensional step-over to the Pyramid Lake fault to the northwest. Second, as the

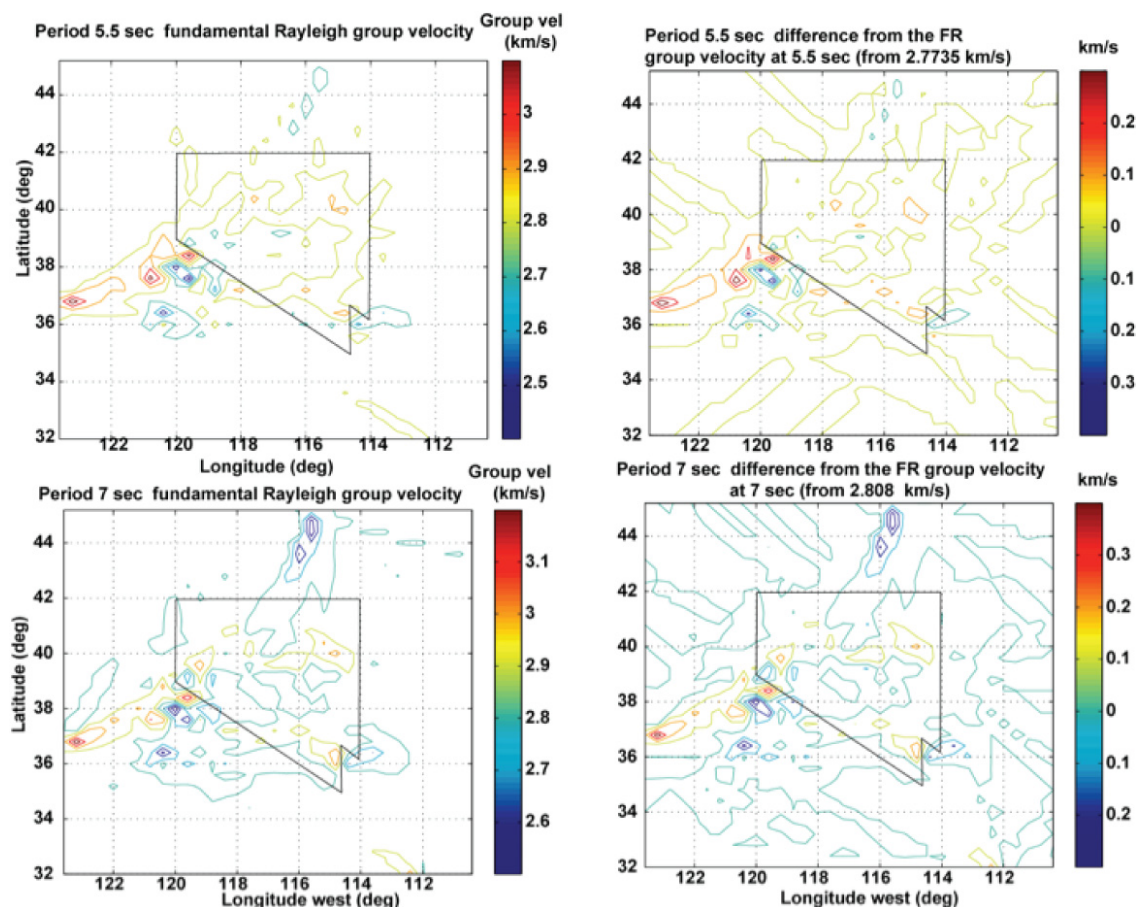


Figure 4. Preliminary tomographic model results at the periods of 5.5 sec and 7 sec. The left plots show contours of the fundamental mode Rayleigh (FR) wave group velocity values at each period. The right plots show differences in fundamental mode Rayleigh wave group velocity from the mean model at the period shown.

basin opens, lower velocity near-surface rocks are dropped deeper in the section. The net effect on seismic velocity will be an apparent low much deeper than the basin depth alone.

We may also observe that while visually underwhelming, a velocity contrast of the order of 3-4% at a given depth is about what one would expect between granite or amphibolite facies granitic rocks and tonalitic or dioritic rocks under similar conditions. Velocities do not automatically map to facies or petrologic differences, but with some care, can be used with geologic and other geophysical data to make improved interpretations.

Surface wave data compliment this interpretational picture because surface waves sample from the surface down, while body waves largely travel beneath the geology sampled by surface waves. Also, surface waves are more sensitive to shear wave velocity than to compressional. This is of value to the geothermal community since shear wave indicators for geothermal effects have larger magnitudes (that is, V_s is affected more by geothermally interesting conditions than is V_p). On the other hand, surface waves have longer wavelengths and fewer are available, so resolution is necessarily lower.

A recently received dataset developed by the Array Network Facility will afford us an opportunity to significantly expand the

body wave coverage presented here. These data include large numbers of located quarry blasts from geothermally important north-central Nevada. Processing and inversion of these data is in work and will be available by the time of the 2010 GRC meeting.

Acknowledgements

This work was supported by the Great Basin Center for Geothermal Energy, U.S. Department of Energy, DE-FG36-02ID14311. Sandia is a multi-program laboratory operated by Sandia Corporation, a Lockheed Martin Company, for the United States Department of Energy's National Nuclear Security Administration under Contract DE-AC04-94AL85000.

References

- Feng, C.-C. and T.-L. Teng, 1983. Three-dimensional crust and upper mantle structure of the Eurasian continent. *J. Geoph. Res.*, 88, 2261-2272.
- Priestley, K. F. and J. N. Brune. (1982). Shear wave structure of the southern Volcanic Plateau of Oregon and Idaho and the northern Great Basin of Nevada from surface wave dispersion, *J. Geoph. Res.*, 87, 2671-2675.